Mechanical stimulation of cervical vertebrae modulates the discharge activity of ventral tegmental area neurons and dopamine release in the nucleus accumbens

Kyle B. Bills[a], **J. Daniel Obray**[a], **Travis Clarke**[a], **Mandy Parsons**[a], **James Brundage**[a], **Chae Ha Yang**[b], **Hee Young Kim**[b], **Jordan T. Yorgason**[a], **Jonathan D. Blotter**[c], **Scott C. Steffensen**[a,*]

[a]Brigham Young University, Department of Psychology/Neuroscience, Provo, Utah, 84602, USA

[b]College of Korean Medicine, Daegu Haany University, Daegu, 42158, South Korea

[c]Brigham Young University, Department of Engineering, Provo, Utah, 84602, USA

Abstract

Background: Growing evidence suggests that mechanical stimulation modulates substrates in the supraspinal central nervous system (CNS) outside the canonical somatosensory circuits.

Objective/Methods: We evaluate mechanical stimulation applied to the cervical spine at the C7-T1 level (termed "MStim") on neurons and neurotransmitter release in the mesolimbic dopamine (DA) system, an area implicated in reward and motivation, utilizing electrophysiological, pharmacological, neurochemical and immunohistochemical techniques in Wistar rats.

Results: Low frequency (45–80 Hz), but not higher frequency (115 Hz), MStim inhibited the firing rate of ventral tegmental area (VTA) GABA neurons (52.8% baseline; 450 s) while increasing the firing rate of VTA DA neurons (248% baseline; 500 s). Inactivation of the nucleus accumbens (NAc), or systemic or *in situ* antagonism of delta opioid receptors (DORs), blocked MStim inhibition of VTA GABA neuron firing rate. MStim enhanced both basal (178.4% peak increase at 60 min) and evoked DA release in NAc (135.0% peak increase at 40 min), which was blocked by antagonism of DORs or acetylcholine release in the NAc. MStim enhanced c-FOS expression in the NAc, but inhibited total expression in the VTA, and induced translocation of DORs to neuronal membranes in the NAc.

Conclusion: These findings demonstrate that MStim modulates neuron firing and DA release in the mesolimbic DA system through endogenous opioids and acetylcholine in the NAc. These findings demonstrate the need to explore more broadly the extra-somatosensory effects of peripheral mechanoreceptor activation and the specific role for mechanoreceptor-based therapies in the treatment of substance abuse.

*Corresponding author. 1050 SWKT, Brigham Young University, Provo, UT, 84602, USA, scott_steffensen@byu.edu (S.C. Steffensen).

Keywords

Dopamine; GABA; Mechanoreceptors; Opioid receptors; VTA; Accumbens

Introduction

The use of mechanoreceptor-based therapies in the treatment of drug-abuse disorders is a largely unexplored field. Indeed, the role of mechanoreceptors other than as canonical mediators of somatosensation has only become relevant in recent years. Notably, several complementary health care approaches are thought to have effects mediated in part by activation of mechanoreceptors, including chiropractic medicine, acupuncture, and physical therapy. Early understanding of the mechanisms underlying mechanoreceptor-based therapies such as WBV centered on peripheral neuro-mechanical alterations. Recent reports have included evidence of increased cortical excitability [1], increased motor evoked potentials [2], and compelling evidence demonstrating CNS changes in response to peripheral mechanical stimulation as measured with fMRI, EEG, heart rate variability, and evoked potentials [1,3,4].

Midbrain dopamine (DA) neuron activity is involved in many aspects of reward seeking [5]. Although the prevailing dogma is that DA neurons mediate the rewarding and addictive properties of drugs of abuse [6], VTA GABA neurons have garnered much interest for their role in modulating DA neuronal activity and DA release and perhaps as independent substrates mediating reward or aversion [7–10]. We have shown previously that acute administration of ethanol, opioids, or cocaine inhibits VTA GABA neurons [7–11], leading to a net disinhibition of VTA DA neurons [12,13]. In contrast, during ethanol or opioid withdrawal, VTA GABA neurons become hyperactive [7,14] leading to decreased mesolimbic DA activity and release in the NAc [15–17], This reduction in mesolimbic DA transmission is theorized to be the primary driver of relapse [18].

In this study, we hypothesized that mechanical stimulation of the cervical spine at C7-T1 (termed "MStim") is sufficient to modulate neuronal activity in the VTA and neurotransmitter release in the NAc. We have recently reported that MStim of the cervical spine modifies the activity of VTA GABA neurons [19]. Here we extend these studies to include the recording of VTA GABA and DA neurons, DA release, and mechanistic studies demonstrating the role of endogenous opioid release in mediating mechanoreceptor activation of the mesolimbic DA system.

Materials and methods

Animals and MStim motor implantation

The experiments were carried out in accordance with the Guide for the Care and Use of Laboratory Animals. Male rats (250–320 g), housed on a reverse light/dark cycle with *ad libitum* food and water, were implanted with a 1.5 g, 3 V, DC coin vibration motor (10 mm × 2.7 mm, DC 3V/0.1A, Uxcell, Hong Kong, CN) [19]at the C7-T1 levels posteriorly at midline or at the ipsilateral biceps femoris muscle. With a S44 Grass Stimulator (Grass Medical

Instruments, West Warwick, RI) set at 3 V for 0.1 msec [19], pulses/sec were varied to produce 45, 80 and 115 Hz vibrations for 60 or 120 s followed by 15 min of recording. The 80 Hz, 120 s stimuli resulted in the greatest inhibition of GABA neuron firing rate and was used in all subsequent testing.

Single cell electrophysiology

For recordings of VTA GABA and DA neurons, rats were anesthetized using isoflurane (1.5%) and body temperature was maintained at 37.4 °C. 3.0 M KCl-filled micropipettes (2–4 MΩ; 1–2 μm inside diameter) were driven into the VTA with a piezoelectric microdrive (EXFO Burleigh 8200 controller and Inchworm, Victor, NY) [from bregma: 5.6 to 6.5 posterior (P), 0.5 to 1.0 lateral (L), 6.5 to 9.0 ventral (V)]. Potentials were amplified with an Multiclamp 700A amplifier (Axon Instruments, Molecular Devices, Union City, CA) and filtered at 0.3–10 kHz (3 dB). Potentials were sampled at 20 kHz and discriminated with a World Precision Instruments WP-121 Spike Discriminator (Sarasota, FL) and converted to computer-level pulses.

Characterization of VTA GABA and DA neurons in vivo

VTA GABA neurons were identified by discharge activity characteristics including: relatively fast firing rate (>10 Hz), ON-OFF phasic non-bursting activity, an initially negative spike with duration less than 200 μsec [20], and excitation by iontophoretic (+40 nA) DA [9,10]. Dopamine neurons were identified by relatively slow firing rate (<10 Hz), an initially positive-going spike of longer than 200 μsec and inhibition by iontophoretic DA. We evaluated only those spikes that had greater than 5:1 signal-to-noise ratio. After positive neuron identification, baseline firing rate was measured for 5 min to ensure stability prior to MStim.

Fast-Scan Cyclic Voltammetry (FSCV) in vivo

A carbon fiber containing borosilicate glass capillary tube (CFE; 1.2 mm o.d., A-M Systems, Sequim, WA, USA) was pulled, cut so that 150–200 μm of fiber was protruding and filled with 3 M KCl. The electrode potential was scanned from −0.4 V to 1.3 V and back at 400 V/s with recordings every 100 msec using Demon Voltammetry [21]. For *in vivo* voltammetry recordings, bipolar, stimulating electrodes were stereotaxically implanted into the medial forebrain bundle (MFB; −2.5 AP, +1.9 ML, −8.0 DV), and a CFE in the NAc (+1.6 AP, +1.9 ML, −8.0 DV). The MFB was stimulated with 60 pulses at 60 Hz (4 msec pulse width) at 2 min intervals until stable for five successive collections, defined as <10% variance. Following MStim, recordings were performed for 120 min or until baseline was reached.

Microdialysis and high performance liquid chromatography

Microdialysis probes (MD-2200, BASI) were stereotactically inserted into the NAc and perfused with artificial cerebrospinal fluid (aCSF) composed of either 150 mM NaCl, 3 mM KCl, 1.4 mM $CaCl_2$, and 0.8 mM $MgCl_2$ in 10 mM phosphate buffer alone or, additionally, with either 10 nM naltrindole or a combination of 10 μM hexamethonium and 10 μM scopolamine (3.0 μl/min). Samples were collected every 20 min for 4 h with MStim

occurring after the first 2 h. Samples were analyzed using a HPLC pump (Ultimate 3000, Dionex, Sunnyvale, CA, USA) and electrochemical detector (Coulochem III, ESA). The detector included a guard cell (5020, ESA) set at +270 mV, a screen electrode (5014B, ESA) set at −100 mV, and a detection electrode (5014B, ESA) set at +220 mV. Dopamine was separated using a C18 reverse phase column (HR-80, Thermo Fisher Scientific, Waltham, MA, USA). Mobile phase included 75 mM H_2NaO_4P, 1.7 mM sodium octane sulfonate, 25 μM EDTA, 0.714 mM triethylamine, and 10% acetonitrile at a flow rate of 0.5 ml/min.

Preparation of brain slices for imaging and confocal microscopy

Mechanical stimulation animals were implanted and given 120 s of 80 Hz stimulation. Control animals were implanted but not stimulated. After 2 h brains were removed and placed in 4% PFA for 24 h, 30% sucrose in 1X PBS for 24–48 h and then flash frozen in dry ice for slicing. Slices were washed 3 times in 1x PBS, blocked with 4% normal goat serum, 0.1% Triton-X 100 and 1x PBS and then washed 3 times in 0.2% PBST. Primary antibodies incubated for 20 h and were washed 3 times. Secondary antibodies incubated for 2 h and were washed 3 times. Slices were mounted and kept at 4 °C until imaging. An Olympus FluoView FV1000 confocal microscope was used to image mounted slices at 40X.

Data collection and statistical analysis

All statistical tests were performed in JMP13 (SAS, Cary, NC). Extracellularly recorded single-unit action potentials were processed with a spike analyzer, digitized with National Instruments hardware and analyzed with National Instruments LabVIEW and IGOR Pro software (Wavemetrics, Lake Oswego, OR). Firing rate was averaged and binned in 50 s intervals and compared to unstimulated neurons using a one-way ANOVA then bins were compared with a Student's t-test. Average depression or excitation was calculated as time firing deviated >10% from baseline. The results were expressed as means ± SEM.

For microdialysis and FSCV data was binned and compared to the baseline control using a Dunnett's analysis. Reverse microdialysis and VTA injection experiments were compared to the MStim group using a Student's t-test at the 60 min time point.

Brain slice images were loaded into FIJI software. Brightness and contrast were adjusted and regions of interest (ROI) were created. To determine relative density of DORs, the ratio of mean fluorescence to area was determined. This process was performed by three blinded independent raters and averaged.

Results

MStim modulation of VTA neurons

The effects of MStim on VTA GABA neuron firing rate were tested across multiple stimulus frequencies and durations (Fig. 1). MStim at 45 Hz (60 s) significantly inhibited GABA neuron firing rate when compared to unstimulated baseline firing ($F_{(1,277)} = 24.9997$, $p < 0.0001$; Fig. 1A). GABA neuron firing rate was significantly reduced from 50 s to 250 s post-stimulus when compared to baseline (n = 4; 50 s, $p = .0216$; 100 s, $p = .0460$; 150 and 200 s, $p < .0001$; 250 s, $p = .0222$). Stimulation at 80 Hz (60 s) ($F_{(1,272)} = 10.1423$, $p =$

0.0016; Fig. 1B) produced GABA inhibition similar to that produced by 45 Hz, with significant depression from 100 to 250 s post-stimulus (n = 5; 100 s, $p = .0186$; 150 and 200 s, $p < .0001$; 250 s, $p = .0101$). MStim effects with the same frequencies at a duration of 120 s are shown in Fig. 1D–F. A 45 Hz stimulation (120 s) significantly inhibited VTA GABA neurons ($F_{(1,282)} = 15.2029$, $p = 0.0001$; Fig. 1D) similar to that observed with 60 s MStim (n = 5, 250 s, $p = .0032$; 300 s, $p < .0001$; 350 s, $p = .0434$). The greatest inhibition to GABA neuron firing rate occurred following application of 80 Hz (120 s) MStim ($F_{(1,296)} = 114.0478$, $p < 0.0001$; Fig. 1E) which produced significant inhibition from 50 to 450 s post-stimulus (n = 7, 50–350 s and 450 s, $p < .0001$; 400 s, $p = .0028$). In contrast, both 60 and 120 s of 115 Hz stimulation (Fig. 1C,F) did not produce a significant depression to GABA neuron firing rate. Thus, GABA neuron firing was inhibited by MStim in a differential and frequency-dependent manner.

Because somatosensory mechanoreceptor density varies by topography [22,23] a location with a relatively smaller concentration of mechanoreceptors was tested. Mechanical stimulation of 80 Hz (120 s) at the belly of the right biceps femoris muscle produced a small decrease in GABA neuron firing rate when compared to C7-T1 ($F_{(1,421)} = 146.4646$, $p < .0001$; Fig. 2A). The two were significantly different at 100–200 and 300 s post-stimulus (n = 4; 100 s, $p = .0137$; 150 s, $p = .0021$), suggesting that MStim-dependent inhibition of VTA GABA firing is greatest at areas of high mechanoreceptor density. Next, the effects of paired MStim was tested on VTA GABA firing rate (Fig. 2B). Compared to the second stimulation, the first typically produced greater inhibition ($F_{(1,411)} = 29.2118$, $p < .0001$). Significant differences were noted at 100–200 s and 300 s (n = 5; 100 s, p = .0137; 150 s, p = .0021; 200 s, .0078; 300 s, p = .0033). Thus, MStim-dependent inhibition of firing rate was repeatable, but sensitive to desensitization-dependent processes.

Since the dogma is that VTA GABA neurons provide inhibitory input onto local DA neurons, the effects of MStim on VTA DA neuron firing was tested. Dopamine neuron firing rate increased significantly post-stimulus ($F_{(1,429)} = 246.4261$, $p < 0.0001$; Fig. 3A) reaching an average maximum increase of 286% of baseline at 150 s post-stimulus. Firing rate increased significantly within the first 50 s and stayed elevated to 500 s post-stimulus. These times points (50–500 s post-stimulus) were all significant when compared to unstimulated baseline DA neuron firing rate over time (n = 5; 50–250 and 350–400 s, $p < .0001$; 300 s, $p = .0026$; 450 s, $p = .0145$; 500 s, p = .0389; Fig. 3B). On average, following MStim, DA neurons increased firing rate to 247% of baseline compared to 52.8% inhibition observed in GABA neurons (Fig. 3C). The increase in DA neuron firing rate occurred in parallel to the reported decrease in GABA neuron firing rate noted from the same stimulation paradigm, suggesting disinhibition of DA neurons from decreased GABA neuron firing.

MStim modulation of VTA neurons: role of NAc projections and endogenous opioids

We have previously demonstrated that stimulation of the NAc inhibits VTA GABA neurons [20], via direct pathway GABAergic medium spiny neurons, and that opiate effects on VTA GABA neuron firing rate are mediated, in part, via GABA input to the VTA from the NAc [11]. To determine if MStim modulation of VTA GABA neurons was in the VTA or via NAc input to the VTA we evaluated the effects of *in situ* administration of the sodium channel

blocker lidocaine into the NAc on MStim effects on VTA GABA neuron firing rate. Inactivation of NAc neurons by perfusion of lidocaine into the NAc via reverse microdialysis blocked MStim-induced depression of VTA GABA firing ($F_{(1,416)}$ = 264.9918, $p < .0001$; n = 5; Fig. 4A). All time points from 50 to 500 s were significantly different (80 Hz 120 s w/ lidocaine injection in NAc, n = 5; 80 Hz 120 s, n = 7; 50 s, $p < .0001$; 100 s, $p < .0001$; 150 s, $p < .0001$; 200 s, $p < .0001$; 250 s, $p < .0001$; 300 s, $p < .0001$; 350 s, $p = .0005$; 400 s, $p < .0001$; 450 s, $p < .0001$; 500 s, $p < .0001$). Next, systemic pretreatment with naltrindole (1 mg/kg IP), 15 min prior to MStim was administered to determine the role of DORs. Naltrindole precluded the depression of GABA neuron firing rate ($F_{(1,487)}$ = 190.4457, $p < .0001$; n = 4; Fig. 4A and B). The depression was blocked at every time point that was previously significant when comparing the 80 Hz stimulus to unstimulated baseline recordings in GABA neurons. The differences between 80 Hz w/naltrindole and 80 Hz alone were pronounced and noted at all time points from 50 to 500 s (80 Hz 120 s w/naltrindole, n = 4; 80 Hz 120 s, n = 7; 50 s, $p < .0001$; 100 s, $p < .0001$; 150 s, $p < .0001$; 200 s, $p < .0001$; 250 s, $p < .0001$; 300 s, $p < .0001$; 350 s, $p = .0017$; 400 s, $p = .0101$; 450 s, $p = .0002$; 500 s, $p < .0001$).

MStim enhancement of dopamine release: role of endogenous opioids

To determine if MStim-induced changes in DA firing translate to an increase in DA neurotransmission, microdialysis and voltammetry experiments were performed. Microdialysis revealed an increase in basal release, with greatest release occurring from 40 to 60 min (178.43 ± 26.24% of baseline), after MStim (n = 15; 60 min, Dunnett's, p = .016; Fig. 5A). From 80 to 120 min post-stimulus, DA levels returned to baseline levels and stabilized. Next, voltammetry experiments were used to measure electrically evoked DA release. Evoked DA release rose slightly faster than basal release with significant increases 10 min post-stimulus (Fig. 5B). Increased levels of evoked DA release were significantly maintained from 10 to 50 min, peaking at 40 min (135.03 ± 23.13% of baseline), with a return to baseline levels at 60 min (n = 4; Dunnett's 10 min, $p = .0176$; 20 min, $p = .0053$; 30 min, $p = .0781$; 40 min, $p = .0006$; 50 min, $p = .0023$). Thus, MStim produces increases in DA levels.

We then evaluated the role of endogenous opioids in mediating MStim-induced enhancement of DA release in the NAc. To determine the site specificity of the DORs involved in the effect (VTA versus NAc) we administered an ipsilateral injection of naltrindole into the VTA 15 min prior to stimulation and found unexpectedly that it did not attenuate MStim-induced DA release in the NAc (n = 15, MStim alone; n = 4, VTA naltrindole; $p = 0.570$). Next, to determine whether local antagonism of NAc DORs contribute to MStim induced increases in DA release, we applied naltrindole via reverse microdialysis (10 nM) in the NAc prior to MStim at the cervical spine (Fig. 6A). Local application of naltrindole blocked the MStim-induced increase in DA release in the NAc at the 60 min time point from 178.43 ± 26.24% of baseline in the MStim alone group to 88.0 ± 9.31% of baseline (n = 15, MStim alone; n = 8, naltrindole NAc; p = .0096; Fig. 6B). As sensory-driven cholinergic interneurons (CINs) in the NAc express DORs and have been shown to influence local DA release [24,25], a combination of hexamethonium (10 μM) and scopolamine (10 μM) was then administered to the NAc via reverse microdialysis to evaluate

the role of local acetylcholine (ACh) release on MStim induced DA release (Fig. 6A). At the 60 min time point DA release increased to $107.62 \pm 3.4\%$ of baseline which represents significant attenuation of the MStim induced DA increase when compared to the MStim alone group (n = 15, MStim alone; n = 8, Hex/Scop NAc; p = .0311; Fig. 6B). These data suggest that the MStim-induced increase in DA release in the NAc is mediated through endogenous activation of DORs in the NAc and not the VTA and that the effect is in part influenced by local release of Ach from CINs.

MStim activation of NAc neurons

To further evaluate neuronal activation changes in the NAc and VTA and alterations in DOR expression in the NAc following MStim, post-MStim brain slices were stained to evaluate changes in relative expression of DORs and c-FOS. The number of cells per slide expressing DORs in the NAc was significantly increased in the MStim group when compared to control ($F_{(1,11)} = 10.6$, $p = 0.008$; n = 6; Fig. 7A,B,E). Expression of c-FOS in the NAc and VTA was analyzed for cell count and mean fluorescent intensity (MFI). The number of cells expressing c-FOS in the NAc increased following MStim (53.0 ± 6.29) when compared to control (33.83 ± 6.79; $p = 0.0314$, n = 6), but not in the VTA (50.50 ± 2.94 vs 65.83 ± 9.36 cells; $p = 0.0847$; Fig. 7C). However, when considering c-FOS MFI, there was a decrease in c-FOS expression in the VTA with MStim ($109.6 \pm 0.9\%$ vs $116.8 \pm 1.2\%$; p = 0.0071, n = 6; Fig. 7D), but not in the NAc. Together, these data suggest that the decrease in VTA c-FOS expression following MStim is likely due to enhanced inhibitory projections from the NAc.

Discussion

Low to high frequency (45–80 Hz) MStim produced robust inhibition of VTA GABA neurons. This was not surprising given our previous reports regarding mechanoreceptor-mediated inhibition of VTA GABA neurons [19,26]. However, here we demonstrated that decreases in VTA GABA neuron firing by MStim are frequency, location, and time-dependent, and are accompanied by concomitant increases in VTA DA cell firing, increases in DA release in the NAc and mediation by endogenous opioid and local ACh release in the NAc. The three frequencies tested were chosen to provide clarity as to the mechanoreceptors responsible for the effect. Of those chosen, 45 Hz enlists mostly Meissner's corpuscles [27], 115 Hz is more selective for Pacinian corpuscles [28,29] and 80 Hz likely activates both receptors. All three frequencies activate Ruffini endings and Golgi tendon organs which are morphologically similar and are important joint mechanoreceptors [30,31]. The 50 and 80 Hz MStim produced a transient depression of GABA neurons in the VTA, with 80 Hz (120 s) producing the largest and longest lasting effect. Importantly, 80 Hz MStim failed to achieve a meaningful depression in VTA GABA neuron firing rate when applied at the biceps femoris muscle. This mid-muscle location was chosen because of its distance from joints and subsequent lower concentration of mechanoreceptors relative to the cervical spine [22,23,29], Given that 80 Hz produced the greatest inhibition, 115 Hz failed to elicit a response and that the mid-muscle stimulation was ineffective at 80 Hz, suggesting a role for deep joint mechanoreceptors and Meissner's corpuscle dependent pathways as main mediators of the resultant GABA depression. Taken together, these data suggest that the effects are only anatomically specific insomuch as anatomical location relates to the

potential for mechanoreceptor recruitment. Even dorsal root ganglion cell bodies have been shown to depolarize in response to mechanical stimulation [32], perhaps enhancing the effects from stimulation to spine. Further, the subcutaneous stimulation provided to the cervical spine is likely to have impacted most of the cervical and some of the thoracic spine, increasing the number of cutaneous and joint receptors activated. Mechanical stimulation at 80 Hz (120 s) elicited DA neuron firing of 247% baseline that occurred simultaneous to the average depression of GABA neurons to 52.8% of baseline (Fig. 3C). This relationship suggests a disinhibition of DA neurons by way of GABA neuron depression.

The present results suggest that mechanoreceptor stimulation results in increases in endogenous opioid release leading to transient modulation to the mesolimbic circuitry. There is a precedence for frequency-dependent release of endogenous opioids. For instance, in rats tolerant to morphine, low frequency (1–15 Hz) transcutaneous electrical nerve stimulation (TENS) was less effective than placebo controls at reducing joint inflammation, suggesting that TENS-alleviated joint inflammation is opioid dependent [33,34]. Also, the effects of low frequency, but not high frequency, TENS are blocked by application of naloxone at doses selective for mu opioid receptors (MORs) and sparing of DORs and KORs [35]. Conversely, administration of the selective DOR antagonist naltrindole blocks the effects of high frequency TENS but spares those of a similar low frequency stimulation, though this effect appears to be isolated to spinal circuits [35]. Further, transcutaneous vagus nerve stimulation at the ear has been shown to alter functional connectivity of the NAc [36]. Taken together, transcutaneous electrical stimulation, which likely depolarizes a broad selection of neuronal structures including local subcutaneous mechanoreceptors, provides greater rationale for the current studies. Delta opioid receptors are located on synaptic terminals of GABA neurons in the VTA and NAc [37] and, of particular relevance to this study, on CINs in the NAc [38]. Additionally, DORs are located in both the VTA and NAc [39,40] and systemic (IP) administration of naltrindole blocked MStim effects on VTA neuron firing rate and DA release in the NAc. Interestingly, MStim-induced increase in NAc DA release was attenuated by selective blockade of DORs with naltrindole in the NAc but not the VTA. Corroboration of the VTA effects being driven by activity in the NAc was confirmed when MStim-induced VTA GABA neuron depression was blocked by local administration of lidocaine into the NAc. In light of the receptor distribution, the site-specific effect of DOR antagonists, the attenuation by NAc lidocaine application, the disparate expression of c-FOS in the NAc and VTA and the congruity of GABA depression and DA excitation (Fig. 4C), these data suggest that VTA effects are mainly resultant from NAc to VTA projections.

Evoked DA release returned to baseline within 60 min while microdialysis showed a more gradual increase, peaking around 60 min post-stimulus (Fig. 5A and B). Interestingly, because GABA and DA neuron firing rates returned to baseline after 464.3 and 366.7 s post-stimulus, respectively, other factors influence the elevation in DA release. This coupled with the fact that DA release was attenuated by blockade of both cholinergic and DORs in the NAc but not the VTA suggests that local factors related to DA terminals are the main drivers of MStim-induced DA release. Dopamine terminals can be modulated independently of activity in cell body regions [24]. Specifically, sensory thalamic projections activate striatal CINs, which drive DA release through nicotinic acetylcholine (ACh) receptor activation (Fig. 8). Further, accumbal DA release has been shown to increase with administration of

DPDPE, a DOR agonist, in a dose-dependent manner with the effects lasting around 60 min *in vivo* when measured with microdialysis [41]. Therefore, it is also possible that MStim induces striatal release onto local DORs to further enhance DA release, as suggested by the near total blockage of MStim-induced DA release with NAc application of naltrindole. In the striatum, DORs exhibit increased levels of membrane translocation on CINs in response to acute cocaine administration, learning events and by activation of D1 receptors [42], This is particularly relevant considering the increased DOR translocation caused by MStim in the NAc. Activation of DORs on striatal CINs can induce hyperpolarization-activated currents that results in burst firing of CINs [42,43], which can, in turn, lead to further release of DA by activation of ACh receptors located on DA terminals. As previously noted, MStim effects on VTA GABA neurons are likely secondary to MStim effects in the NAc and changes in DA release are likely through changes in CIN circuit effects, local activation of DORs and reciprocal projections from the NAc to VTA. It is also unknown if other non-GABA effects are contributing to MStim-induced increases in DA release.

Mechanoreceptors are among the least understood receptors, including their extra-somatosensory activation effects and even some basic aspects of their signal transduction. In spite of this, it is becoming increasingly evident that mechanoreceptors play a broader role than simply as somatosensory relay devices [44,45]. Here we begin exploration of their effects on mesolimbic circuitry. The mesolimbic DA system is a therapeutic target of treatments for a myriad of conditions including depression, ADHD, eating disorders, Parkinson's and addiction and there is a pressing need for new treatment approaches. Future studies should explore the possibility that practitioners of manual medicine, chiropractic physicians, acupuncturists, and physical therapists, might play in the development and implementation of adjunctive treatments for drug-abuse disorders. Further, though these findings are specific to neurons in one circuit, they open the possibility that translational findings in other brain regions could lead to novel applications for mechanoreceptor-based therapies.

Acknowledgements/author contributions

References

[1]. Krause A, Gollhofer A, Freyler K, Jablonka L, Ritzmann R. Acute corticospinal and spinal modulation after whole body vibration. J Musculoskelet Neuronal Interact 2016;16(4):327–38. [PubMed: 27973385]

[2]. Mileva KN, Bowtell JL, Kossev AR. Effects of low-frequency whole-body vibration on motor-evoked potentials in healthy men. Exp Physiol 2009;94(1):103–16. [PubMed: 18658234]

[3]. Zhang N, Fard M, Bhuiyan MHU, Verhagen D, Azari MF, Robinson SR. The effects of physical vibration on heart rate variability as a measure of drowsiness. Ergonomics 2018:1–19.

[4]. Satou Y, Ishitake T, Ando H, et al. Effect of short-term exposure to whole body vibration in humans: relationship between wakefulness level and vibration frequencies. Kurume Med J 2009;56(l-2):17–23. [PubMed: 20103997]

[5]. Dalle Grave R, Calugi S, Marchesini G. Compulsive exercise to control shape or weight in eating disorders: prevalence, associated features, and treatment outcome. Compr Psychiatr 2008;49(4):346–52.

[6]. Wise RA. Dopamine and reward: the anhedonia hypothesis 30 years on. Neurotox Res 2008;14(2–3):169–83. [PubMed: 19073424]

[7]. Gallegos RA, Criado JR, Lee RS, Henriksen SJ, Steffensen SC. Adaptive responses of GABAergic neurons in the ventral tegmental area to chronic ethanol. J Pharmacol Exp Ther 1999;291:1045–53. [PubMed: 10565823]

[8]. Steffensen SC, Walton CH, Hansen DM, Yorgason JT, Gallegos RA, Criado JR. Contingent and non-contingent effects of low-dose ethanol on GABA neuron activity in the ventral tegmental area. Pharmacol Biochem Behav 2009;92(1):68–75. [PubMed: 18996142]

[9]. Ludlow KH, Bradley KD, Allison DW, et al. Acute and chronic ethanol modulate dopamine D2-subtype receptor responses in ventral tegmental area GABA neurons. Alcohol Clin Exp Res 2009;33(5):804–ll. [PubMed: 19298327]

[10]. Steffensen SC, Taylor SR, Horton ML, et al. Cocaine disinhibits dopamine neurons in the ventral tegmental area via use-dependent blockade of GABA neuron voltage-sensitive sodium channels. Eur J Neurosci 2008;28(10):2028–40. [PubMed: 19046384]

[11]. Steffensen SC. Stobbs SH, Colago EE, et al. Contingent and non-contingent effects of heroin on mu-opioid receptor-containing ventral tegmental area GABA neurons. Exp Neurol 2006;202(1):139–51. [PubMed: 16814775]

[12]. Carboni E, Imperato A, Perezzani L, Di Chiara G. Amphetamine, cocaine, phencyclidine and nomifensine increase extracellular dopamine concentrations preferentially in the nucleus accumbens of freely moving rats. Neuroscience 1989;28(3):653–61. [PubMed: 2710338]

[13]. Bocklisch C, Pascoli V, Wong JC, et al. Cocaine disinhibits dopamine neurons by potentiation of GABA transmission in the ventral tegmental area. Science 2013;341(6153):1521–5. [PubMed: 24072923]

[14]. Bonci A, Williams JT. Increased probability of GABA release during withdrawal from morphine. J Neurosci 1997;17:796–803. [PubMed: 8987801]

[15]. Koeltzow TE, White FJ. Behavioral depression during cocaine withdrawal is associated with decreased spontaneous activity of ventral tegmental area dopamine neurons. Behav Neurosci 2003;117(4):860–5. [PubMed: 12931970]

[16]. Karkhanis AN, Huggins KN, Rose JH, Jones SR. Switch from excitatory to inhibitory actions of ethanol on dopamine levels after chronic exposure: role of kappa opioid receptors. Neuropharmacology 2016;110:190–7. [PubMed: 27450094]

[17]. Wise RA. Dopamine, learning and motivation. Nat Rev Neurosci 2004;5(6):483–94. [PubMed: 15152198]

[18]. Lyness WH, Smith FL. Influence of dopaminergic and serotonergic neurons on intravenous ethanol self-administration in the rat. Pharmacol Biochem Behav 1992;42(1):187–92. [PubMed: 1388276]

[19]. Bills KB, Clarke T, Major GH, et al. Targeted subcutaneous vibration with single-neuron electrophysiology as a novel method for understanding the central effects of peripheral vibrational therapy in a rodent model. Dose Response 2019;17(1). 1559325818825172. [PubMed: 30728758]

[20]. Steffensen SC, Svingos AL, Pickel VM, Henriksen SJ. Electrophysiological characterization of GABAergic neurons in the ventral tegmental area. J Neurosci 1998;18(19):8003–15. [PubMed: 9742167]

[21]. Yorgason JT, Espana RA, Jones SR. Demon voltammetry and analysis software: analysis of cocaine-induced alterations in dopamine signaling using multiple kinetic measures. J Neurosci Methods 2011;202(2):158–64. [PubMed: 21392532]

[22]. McLain RF. Mechanoreceptor endings in human cervical facet joints. Spine 1994;19(5):495–501 (Phila Pa 1976). [PubMed: 8184340]

[23]. McLain RF, Raiszadeh K. Mechanoreceptor endings of the cervical, thoracic, and lumbar spine. Iowa Orthop J 1995;15:147–55. [PubMed: 7634025]

[24]. Yorgason JT, Zeppenfeld DM, Williams JT. Cholinergic interneurons underlie spontaneous dopamine release in nucleus accumbens. J Neurosci 2017;37(8):2086–96. [PubMed: 28115487]

[25]. Threlfell S, Lalic T, Platt NJ, Jennings KA, Deisseroth K, Cragg SJ. Striatal dopamine release is triggered by synchronized activity in cholinergic interneurons. Neuron 2012;75(l):58–64. [PubMed: 22794260]

[26]. Yang CH, Yoon SS, Hansen DM, et al. Acupuncture inhibits GABA neuron activity in the ventral tegmental area and reduces ethanol self-administration. Alcohol Clin Exp Res 2010;34(12):2137–46. [PubMed: 20860620]

[27]. Macefield VG. Physiological characteristics of low-threshold mechanoreceptors in joints, muscle and skin in human subjects. Clin Exp Pharmacol Physiol 2005;32(1–2):135–44. [PubMed: 15730450]

[28]. Biswas A, Manivannan M, Srinivasan MA. Vibrotactile sensitivity threshold: nonlinear stochastic mechanotransduction model of the pacinian corpuscle. IEEE Trans Haptics 2015;8(1):102–13. [PubMed: 25398183]

[29]. Zelena J The development of Pacinian corpuscles. J Neurocytol 1978;7(1):71–91. [PubMed: 632855]

[30]. Vega JA, Garcia-Suarez O, Montano JA, Pardo B, Cobo JM. The Meissner and Pacinian sensory corpuscles revisited new data from the last decade. Microsc Res Tech 2009;72(4):299–309. [PubMed: 19012318]

[31]. Vega JA, Haro JJ, Del Valle ME. Immunohistochemistry of human cutaneous Meissner and pacinian corpuscles. Microsc Res Tech 1996;34(4):351–61. [PubMed: 8807618]

[32]. Viatchenko-Karpinski V, Gu JG. Mechanical sensitivity and electrophysiological properties of acutely dissociated dorsal root ganglion neurons of rats. Neurosci Lett 2016;634:70–5. [PubMed: 27720807]

[33]. Sluka KA. Systemic morphine in combination with TENS produces an increased antihyperalgesia in rats with acute inflammation. J Pain 2000;1(3):204–11. [PubMed: 14622619]

[34]. Sluka KA, Judge MA, McColley MM, Reveiz PM, Taylor BM. Low frequency TENS is less effective than high frequency TENS at reducing inflammation-induced hyperalgesia in morphine-tolerant rats. Eur J Pain 2000;4(2):185–93. [PubMed: 10957699]

[35]. Kalra A, Urban MO, Sluka KA. Blockade of opioid receptors in rostral ventral medulla prevents antihyperalgesia produced by transcutaneous electrical nerve stimulation (TENS). J Pharmacol Exp Ther 2001;298(1):257–63. [PubMed: 11408550]

[36]. Wang Z, Fang J, Liu J, et al. Frequency-dependent functional connectivity of the nucleus accumbens during continuous transcutaneous vagus nerve stimulation in major depressive disorder. J Psychiatr Res 2018;102:123–31. [PubMed: 29674268]

[37]. Trigo JM, Martin-Garcia E, Berrendero F, Robledo P, Maldonado R. The endogenous opioid system: a common substrate in drug addiction. Drug Alcohol Depend 2010;108(3):183–94. [PubMed: 19945803]

[38]. Britt JP, McGehee DS. Presynaptic opioid and nicotinic receptor modulation of dopamine overflow in the nucleus accumbens. J Neurosci 2008;28(7):1672–81. [PubMed: 18272687]

[39]. Margolis EB, Fujita W, Devi LA, Fields HL. Two delta opioid receptor subtypes are functional in single ventral tegmental area neurons, and can interact with the mu opioid receptor. Neuropharmacology 2017;123:420–32. [PubMed: 28645621]

[40]. Hipolito L, Sanchez-Catalan MJ, Zanolini I, Polache A, Granero L. Shell/core differences in mu- and delta-opioid receptor modulation of dopamine efflux in nucleus accumbens. Neuropharmacology 2008;55(2):183–9. [PubMed: 18582908]

[41]. Hirose N, Murakawa K, Takada K, et al. Interactions among mu- and delta-opioid receptors, especially putative delta1- and delta2-opioid receptors, promote dopamine release in the nucleus accumbens. Neuroscience 2005;135(1):213–25. [PubMed: 16111831]

[42]. Bertran-Gonzalez J, Laurent V, Chieng BC, Christie MJ, Balleine BW. Learning-related translocation of delta-opioid receptors on ventral striatal cholinergic interneurons mediates choice between goal-directed actions. J Neurosci 2013;33(41):16060–71. [PubMed: 24107940]

[43]. Laurent V, Bertran-Gonzalez J, Chieng BC, Balleine BW. delta-opioid and dopaminergic processes in accumbens shell modulate the cholinergic control of predictive learning and choice. J Neurosci 2014;34(4):1358–69. [PubMed: 24453326]

[44]. Feland JB, Hawks M, Hopkins JT, Hunter I, Johnson AW, Eggett DL. Whole body vibration as an adjunct to static stretching. Int J Sports Med 2010;31(8):584–9. [PubMed: 20535662]

[45]. Tseng SY, Hsu PS, Lai CL, Liao WC, Lee MC, Wang CH. Effect of two frequencies of whole-body vibration training on balance and flexibility of the elderly: a randomized controlled trial. Am J Phys Med Rehabil 2016;95(10):730–7. [PubMed: 27088462]

Author Manuscript

Author Manuscript

Author Manuscript

Author Manuscript
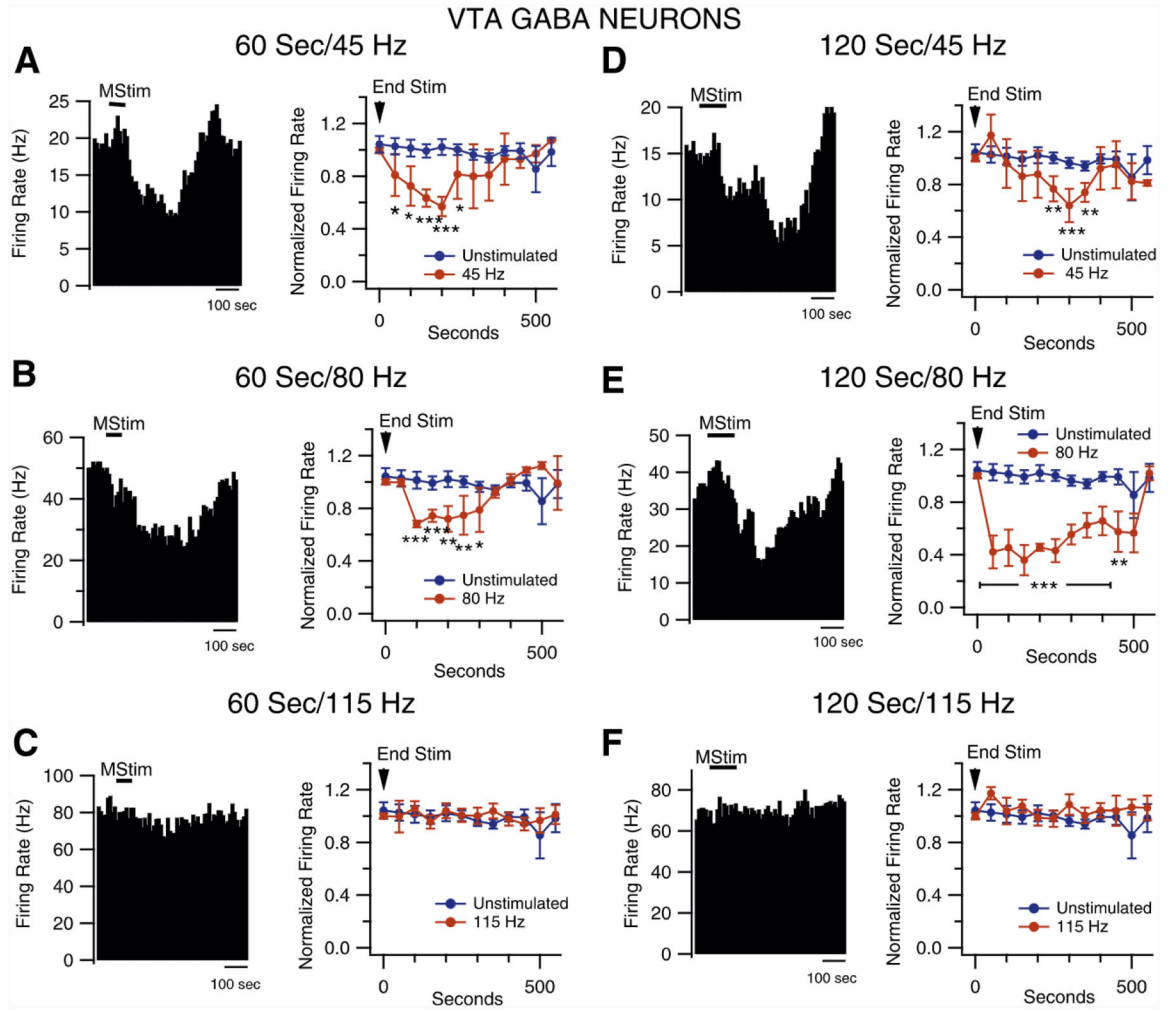
Fig. 1.
Frequency and duration-dependent effects of MStim on VTA GABA neuron firing rate. (A–C) Summarized time course data for 45 (A), 80 (B) and 115 Hz (C) stimulation at 60 s duration. Representative ratemeter recordings of VTA GABA neurons are shown on the left and summarized data on the right. Note that 45 and 80 Hz MStim significantly inhibited the firing rate of VTA GABA neurons while 115 Hz had no effect. (D–F) The same set of frequency responses, but with a 120 s stimulation. Note that 45 and 80 Hz MStim significantly inhibited VTA GABA neuron firing rate while 115 Hz had no effect, and that the inhibition was more pronounced with longer MStim durations. Asterisks *,**,*** indicate significance levels $p < 0.05$, 0.01 and 0.001, respectively.
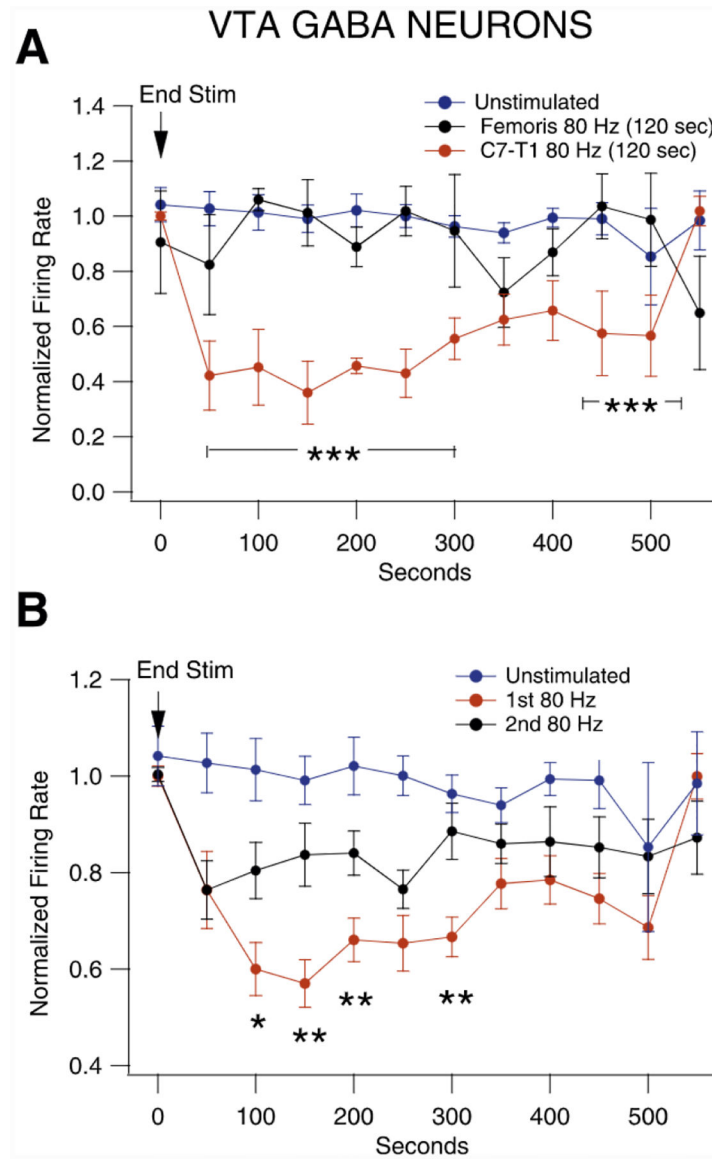
Fig. 2.
Spatiotemporal variation in MStim-induced effects on VTA GABA neuron firing rate. (A) VTA GABA neuron response to MStim (80 Hz; 120 s) at the right biceps femoris muscle belly compared to cervical spine at C7-T1. Note that MStim at the biceps femoris was without effect on VTA GABA neuron firing rate. (B) VTA GABA neuron response to MStim at the C7-T1 vertebral level by two subsequent stimuli. Note the diminution in VTA GABA neuron firing rate with the second 80 Hz, 120 s stimulation compared to the first. Asterisks *,**,*** indicate significance levels $p < 0.05$, 0.01 and 0.001, respectively.
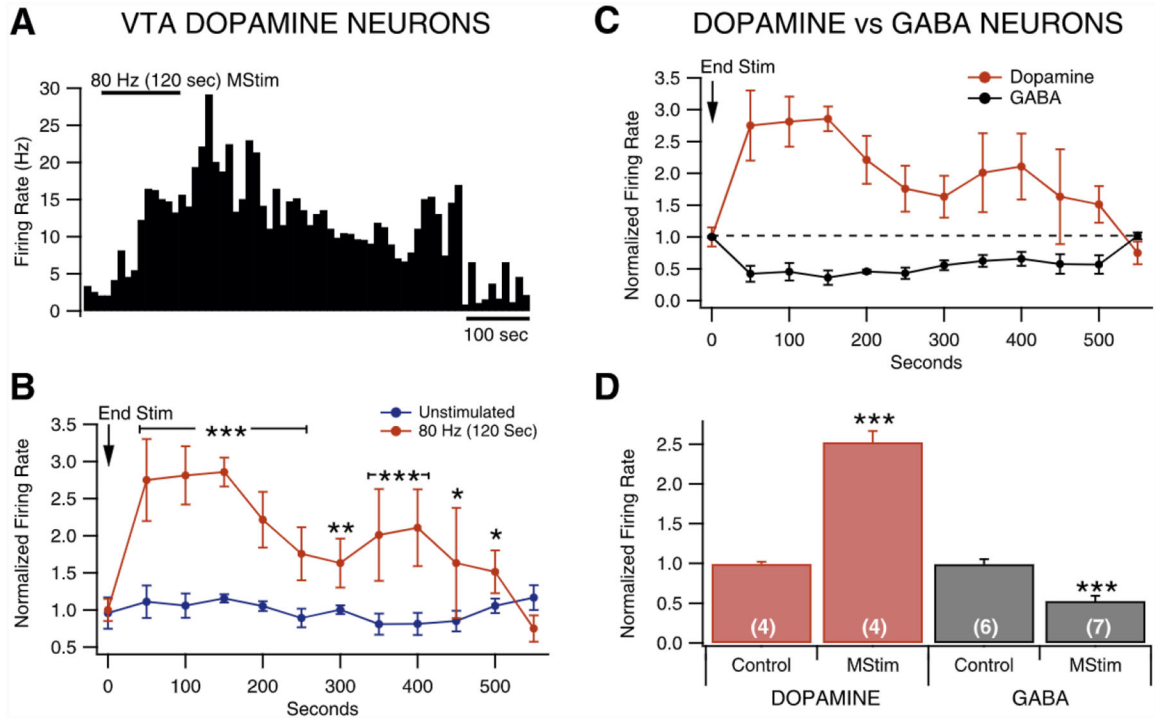
Fig. 3.
Dopamine neuron response to MStim. (A) Representative trace of DA neuron firing rate in response to MStim (80 Hz; 120 s). Note that MStim markedly increased the firing rate of this VTA DA neuron. (B) Summarized time course comparing VTA DA neuron firing rate to MStim vs an unstimulated baseline. (C) Dopamine neuron firing rate changes compared to time-equivalent GABA neuron firing rate changes in response to MStim. (D) Summarized data comparing average firing rate changes in VTA neurons by MStim. Values in parentheses are n values. Asterisks *,**,*** indicate significance levels $p < 0.05$, 0.01 and 0.001, respectively.
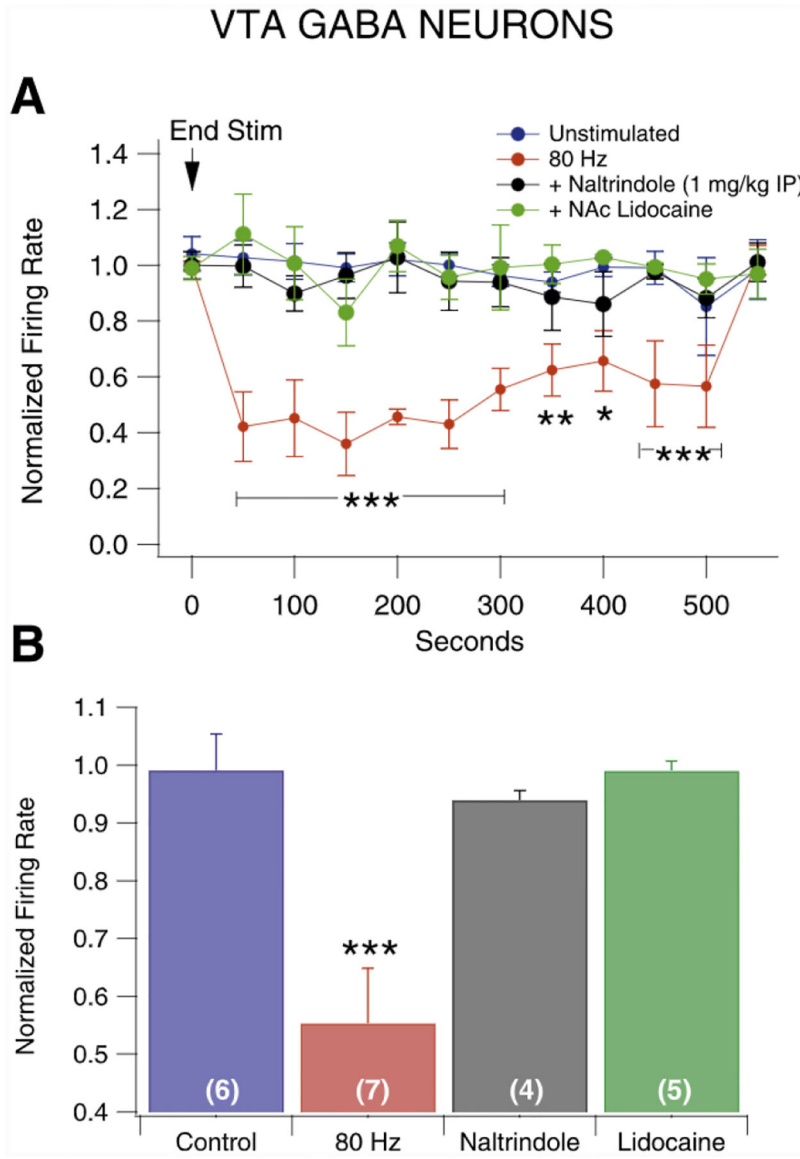
Fig. 4.
Role of NAc inputs to the VTA and endogenous opioids in MStim-induced inhibition of VTA GABA neuron firing rate. (A,B) Local injection of lidocaine into the NAc and IP administration of the DOR antagonist naltrindole blocked MStim-induced inhibition of VTA GABA neuron firing rate (80 Hz; 120 s). Values in parentheses are n values. Asterisks *,**,*** indicate significance levels $p < 0.05$, 0.01 and 0.001, respectively.
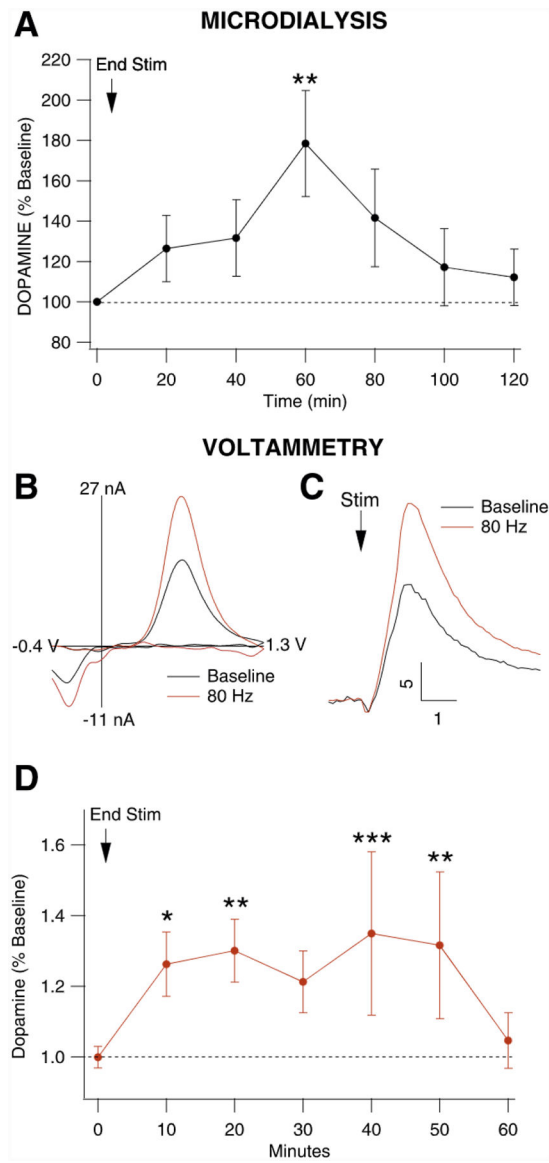
Fig. 5.
MStim effects on basal and evoked DA release in the NAc. (A) MStim enhanced basal DA release in the NAc. as measured by microdialysis. (B) Representative, superimposed voltammograms showing oxidation/reduction current vs voltage plots comparing DA release during baseline vs MStim. (C) Representative, superimposed current vs time plots showing DA release associated with local electrical stimulation. Calibration bars are nA and seconds. (D) MStim also enhanced evoked DA release in the NAc, as measured by voltammetry. Asterisks *,**,*** indicate significance levels $p < 0.05, 0.01$ and 0.001, respectively.
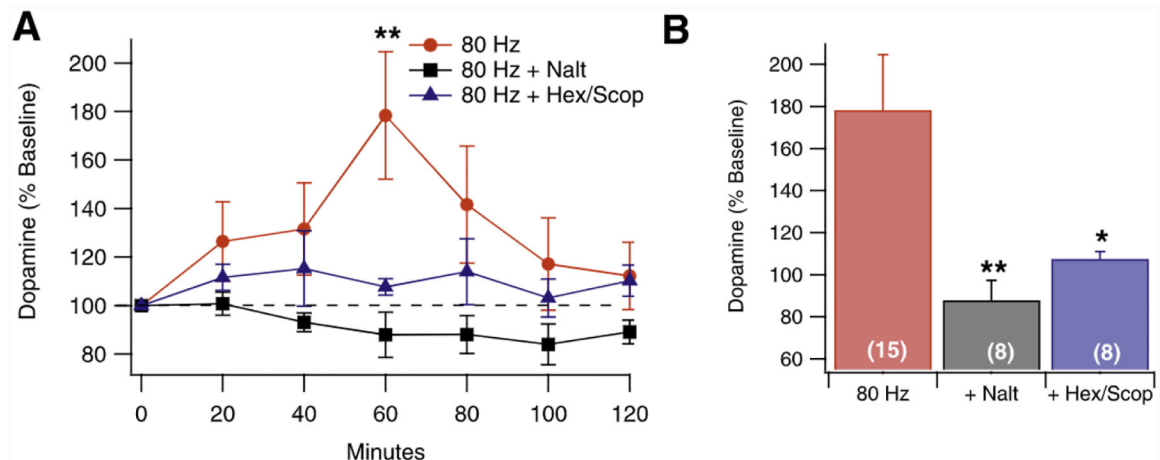
Fig. 6.
Role of DORs and CINs in MStim-induced enhancement of DA release in the NAc. (A) Summarized time course of *in situ* NAc naltrindole or hexamethonium/scopolamine effects on MStim-induced enhancement of basal DA release in the NAc (80 Hz; 120 s). Note that naltrindole or hexamethonium/scopolamine infusion into the NAc blocked MStim-induced enhancement of basal DA release. (B) Summarized data at the 60-min time point. Values in parentheses are n values. Asterisks *,**,*** indicate significance levels $p < 0.05$, 0.01, and 0.001, respectively.
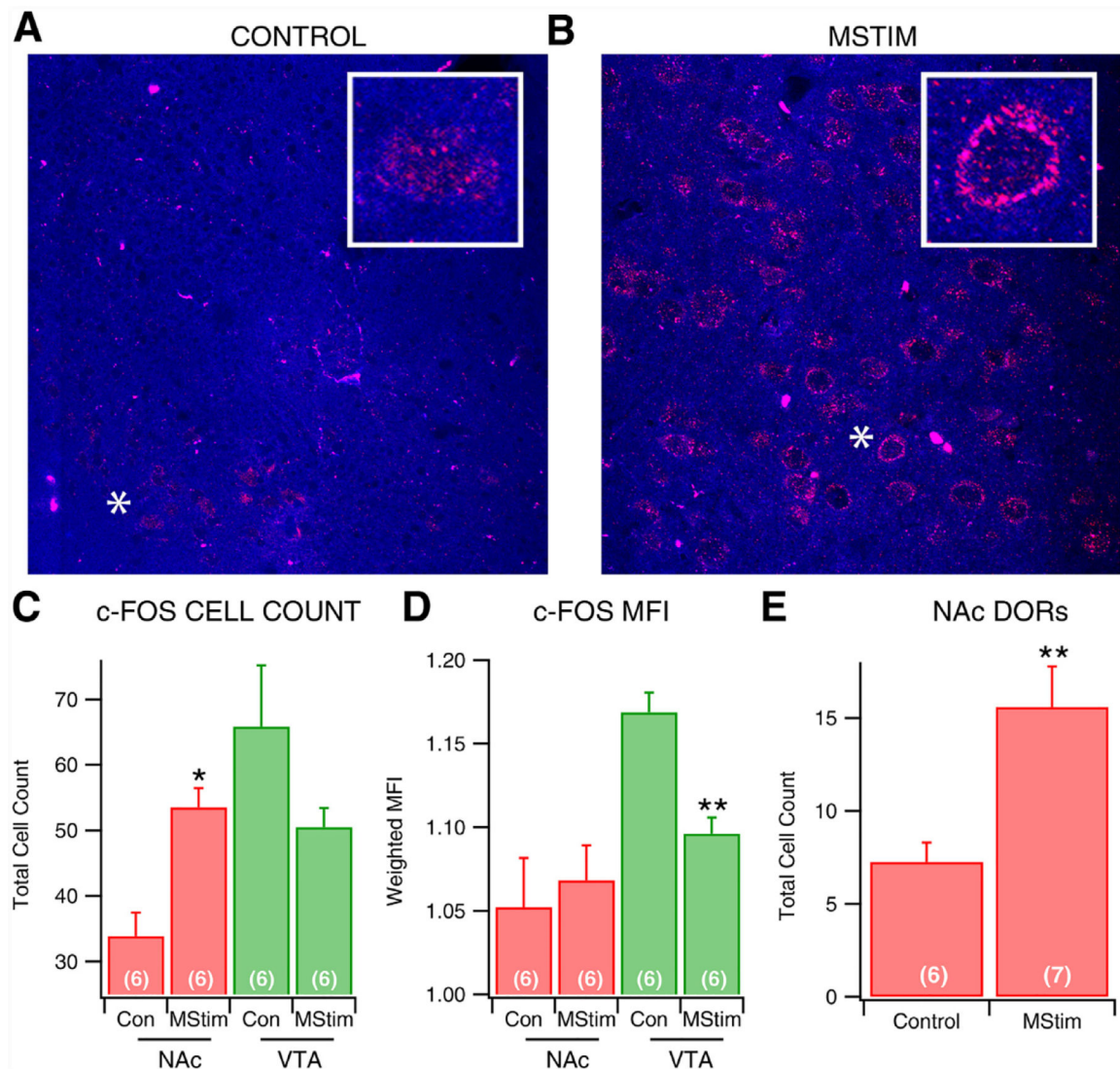
Fig. 7.
MStim activates neurons and induces translocation of DORs in the NAc. (A,B) Increased expression of DORs (red; TH is blue) in the NAc 2-h post MStim compared to control. Insets show magnified views at point on 40X image indicated by the *. Note the translocation of DORs to the cell membrane. (C) Increased number of neurons in the NAc, but not the VTA, expressing c-FOS 2 h post MStim. (D) Decreased expression of c-FOS mean fluorescent intensity (MFI) in the VTA, but not in the NAc, 2 h post MStim. (E) Total number of NAc cells expressing DORs 2 h post MStim. Values in parentheses are n values. Asterisks *,** indicate significance levels $p < 0.05$ and 0.01, respectively.
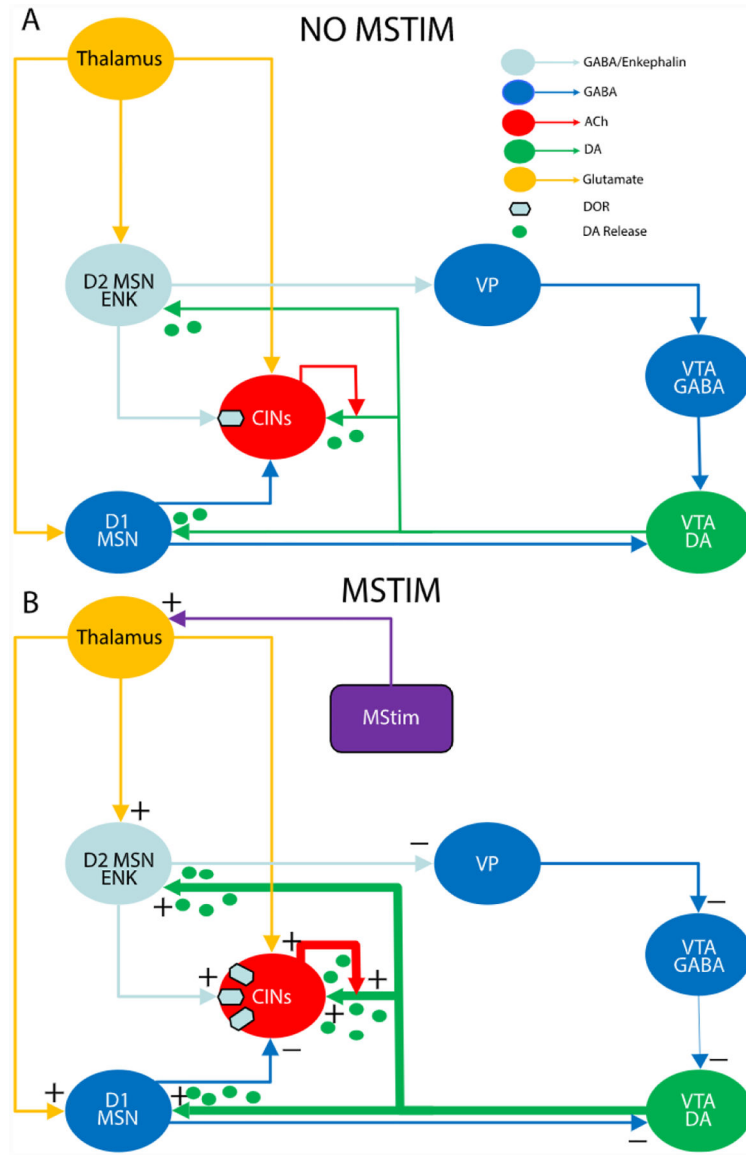
Fig. 8.

Proposed model for MStim effects on striatal neurons. (A,B) DA neurons in the VTA project to the NAc. Dopamine release is also modulated independent of cell body firing at DA terminals in the NAc by CINs. Mechanical stimulation is believed to activate sensory thalamic projections that excite NAc MSNs in both the direct and indirect pathways. D2 MSNs co-release enkephalin and GABA and are thought to be responsible for driving increased NAc C1N activity by hyperpolarization rebound firing via activation of DORs which results in increased DA release. Higher DA release results in increased translocation of DORs to CIN cell membranes creating a longer lasting cycle of MStim-induced DA release. D2 MSNs also project to VTA GABA neurons causing their depression and subsequent disinhibition of VTA DA cell bodies.